electronics

MDPI

Article

Mapping Matrix Design and Improved Belief Propagation Decoding Algorithm for Rate-Compatible Modulation

Jinkun Zhu, Zhipeng Pan, Wei Liu *, Jing Lei and Wei Li

Department of Cognitive Communication; National University of Defense Technology, Changsha 410073, China; zhujinkun@hotmail.com (J.Z.); panzhipeng10@nudt.edu.cn (Z.P.); leijing@nudt.edu.cn (J.L.); liwei.nudt.cn@gmail.com (W.L.)

* Correspondence: wliu_nudt@nudt.edu.cn

Received: 26 January 2019; Accepted: 4 March 2019; Published: 11 March 2019

Abstract: Rate-compatible modulation (RCM) can achieve adaptive transmission in a variable channel environment. However, there are two problems with conventional RCM. Firstly, there is a large number of four rings in the mapping matrix of the conventional RCM, which blocks the delivery of messages in the decoding. Secondly, in the conventional decoding of RCM, the soft information of the last decoding will be discarded when cyclic redundancy check (CRC) is failed, which decreases the performance significantly. In order to address these two problems, in this paper, we propose a new method to construct a mapping matrix without four rings (MMwoFR) and an improved belief propagation (IBP) algorithm for RCM decoding. On the one hand, by using MMwoFR, the constructed matrix is able to prevent the existence of four rings which have much side influence of reliability performance. On the other hand, the IBP is able to make the most use of the soft information in RCM decoding. Simulation results show that using MMwoFR and IBP can bring at least 12% goodput gain for RCM at the high signal-to-noise ratio (SNR) region while maintaining the same performance in the low and moderate SNR regions. Moreover, complexity analysis shows that the new scheme has comparable complexity compared with a conventional RCM.

Keywords: modulation; RCM; rate adaptation

1. Introduction

High transmission rate is an important parameter in wireless communications over time-varying channels. Adaptive coding and modulation (ACM) is an effective way to achieve high transmission rate, which has been adopted in 802.11a [1,2]. However, there are two disadvantages in ACM. Firstly, the sender selects best combination scheme of modulation and coding according to the estimation of the channel conditions, which can be a really tough work for accurate estimation in time-varying channels. Secondly, since ACM only has limited choices of rate combination schemes, the adaptive rate is a stair-case. Superposition coded modulation (SCM) [3] is another coding and modulation scheme. It provides a flexible rate adaptive approach. However, adjusting the rate in SCM still depends on the channel condition.

In order to achieve seamless transmission and overcome the problem of channel estimation at the same time, several rateless codes [4–7] have been proposed. Luby Transform (LT) codes [4] which are originally designed for binary erasure channel (BEC) have unfavorable performance in the Gaussian channel. Raptor codes [6] which are an extension of an LT code simply consist of the concatenation of an LT code with an outer code, called precode, which is usually a high rate error correcting code. The overhead of LT code is large in the Gaussian channel. Due to the overhead and the

outer code rate, the performance of Raptor codes is also unfavorable [8]. Spinal codes [6] is also one of rateless codes which has good performance. However, the complexity of polynomial decoding is a big problem in practical communication systems. Analog fountain codes (AFC) [7], which uses low-density parity-check (LDPC) codes as a precoder, is able to achieve significant performance improvements. However, the design of AFCs is complicated and the complexity of decoding is high.

Rate compatible modulation (RCM) is one of the promising adaptation technologies, which is proposed in [8]. RCM which can achieve seamless adaptation is insensitive to estimation error of channel information and has high spectrum utilization at medium to high SNR. In RCM, the transmitter transfers information bits to symbols based on the mapping matrix and sends symbols continuously. The receiver continuously decode the source bits based on the received symbols until the source bits pass the CRC. After that, an ACK signal acts as a feedback to notify the transmitter starting to transmit symbols generated by another block of bits. In this way, RCM is able to achieve seamless rate adaptation under time-varying channel conditions.

Until now, the study of the RCM has mainly focused on decoding algorithms and practical applications. In [9–12], low complexity decoding algorithms are proposed which can effectively reduce the hardware implementation complexity. In [13], arithmetic bit-interleaved coded modulation (A-BICM) which cascaded LDPC codes is proposed. In [14], Duan et al. proposed a low peak to average power ratio (PAPR) constellation mapping scheme. In [15], a scheme for switching weight sets of RCM according to channel conditions is proposed. Due to the advantages of RCM, RCM has been applied in these areas including visible light communications [16] and multiple access for machine-to-machine communications [17].

However, there are still some problems in RCM . One is that the conventional mapping matrix has a large number of four rings. The existence of four rings will decrease the reliability performance of RCM. Another problem of RCM is that the process of iterative decoding loses lots of useful information. In the conventional RCM system, the receiver discards soft information each time the CRC of the source bits is failed i.e., decoding unsuccessfully. However, the discarded information can be reused in the next decoding process.

LDPC codes [18] have been widly studied to solve the problem that the check matrix has four rings. Quasi-cyclic LDPC (QC-LDPC) codes are a particularly important class of LDPC codes. The finite geometries method [19] or the circulant permutation matrix method [20,21] are the two construction methods of QC-LDPC codes, which are able to generate a check matrix without four rings. Therefore, the design RCM mapping matrix can combine the construction method of QC-LDPC codes.

In this paper, our main aim is to solve these two problems of RCM. We will propose a new method to construct the mapping matrix without four rings (MMwoFR). Specifically, the proposed construction method combines the construction method of QC-LDPC codes. In this proposed construction method, elementary matrix of mapping matrix has been changed and the distribution of the weights of the mapping matrix has been redesigned. Besides, we will present an improved belief propagation (IBP) algorithm for RCM decoding to make the most use of the soft information of the last unsuccessful decoding. In addition, we find that not all the output soft information of the last unsuccessful decoding can be used to help the next decoding. Therefore, the thresholds of the soft information are set to retain the useful soft information.

The rest of the paper is organized as follows. Section 2 reviews the original RCM. Section 3 presents a new mapping matrix construction method. Section 4 proposes an improved belief propagation (IBP) and analyzes the threshold of soft information. Simulations are performed in Section 5. In the Section 6, a conclusion of the paper is made.

2. Original Rate Compatible Modulation

In RCM, source bits are directly mapped to symbols. RCM symbols are generated by arithmetic summation of weighted source bits. $\boldsymbol{x} = (x_1, x_2, x_3, \cdots, x_N)^{\mathrm{T}} \in \{0,1\}^N$ is a vector of source bits and the length of $\boldsymbol{x}$ is N. $\boldsymbol{W_s} = \{w_l | l = 1 \cdots L\}$ is the weights set of RCM. The transmitter randomly selects

L source bits from $\boldsymbol{x}$. These selected bits are part of a weighted arithmetic summation to generate an encoded symbol s_i as Equation (1),

$$s_i = \sum_{l=1}^{L} w_l x_{i_l}, \tag{1}$$

where $w_l \in W_s$ and the subscript i_l is the index of the bit corresponding to the weight w_l. When the number of the transmitted symbols is M, the encoding process can be represented in matrix form $\boldsymbol{s} = \boldsymbol{G}\boldsymbol{x}$, where $\boldsymbol{G}$ denotes the $M \times N$ mapping matrix and $\boldsymbol{s}$ is the symbol vector of length M. In RCM, every two consecutive symbols create one complex-valued symbol u_n as Equation (2),

$$u_n = s_{2n-1} + i \cdot s_{2n}, n > 0, \tag{2}$$

where i is the imaginary unit and $s_{2n-1}, s_{2n} \in \boldsymbol{s}$. In original RCM, $W_s = \{\pm 1, \pm 2, \pm 4, \pm 4\}$. Therefore, the generated symbol is $[-11, 11]$. The constellation map corresponding to the transmitted complex-valued symbol is a 23×23 rectangular constellation point map. The construction of the mapping matrix is very crucial. The construction method of the original RCM mapping matrix takes three constraints as construction critera (more details can be found in [8]).

1. The mapping matrix should be regular in rows.
2. The mapping matrix should be as regular as possible in columns.
3. The weight set is able to create diverse symbol values.

In [8], three steps are taken to construct the mapping matrix. The first step is constructing the elementary matrix. $C(q)$ is a $N/8 \times N/4$ matrix as Equation (3), where q is a variable.

$$C(q) = \begin{bmatrix} +q & -q & & & & & \\ & & +q & -q & & & \\ & & & & \ddots & & \\ & & & & & +q & -q \end{bmatrix}_{N/8 \times N/4.} \tag{3}$$

According to the weight set of RCM, q is 1, 2 or 4. Therefore, three kinds of elementary matrices are constructed including $C(1), C(2)$, and $C(4)$. For these three matrices, the only difference is the value of elements.

The second step is randomly permuting the columns of the three elementary matrices expressed as $\pi(C(1)), \pi(C(2)), \pi(C(4))$. Then, we construct an $N/2 \times N$ matrix G_0 as Equation (4):

$$G_0 = \begin{pmatrix} \pi(C(4)) & \pi(C(4)) & \pi(C(2)) & \pi(C(1)) \\ \pi(C(2)) & \pi(C(1)) & \pi(C(4)) & \pi(C(4)) \\ \pi(C(4)) & \pi(C(4)) & \pi(C(1)) & \pi(C(2)) \\ \pi(C(1)) & \pi(C(2)) & \pi(C(4)) & \pi(C(4)) \end{pmatrix} \tag{4}$$

where $\pi(\cdot)$ represents the process of random permutation of columns of a matrix and $\pi(\cdot)$ is different each time. A plurality of kinds of G_0 can be obtained by using the above method.

The third step is superimposing G_0 of different numbers to obtain the mapping matrix G. In RCM, the mapping matrix is negotiated by the transmitter and the receiver. Generally, two G_0 are superimposed to construct a mapping matrix.

However, the construction method has a problem that the mapping matrix has a large number of four rings. The existence of four rings will affect the performance during decoding. In the actual process, we did the following experiment. Using the original method to construct the mapping matrix 1000 times, the average number of four rings is 729.34.

3. Mapping Matrix Construction Method

In this section, we will introduce a new method to construct the mapping matrix without four rings (MMwoFR). The design of MMwoFR aims at eradicating the four rings and satisfying the three constraints of RCM. Using the new construction method to construct a mapping matrix $G_{new} \in \mathbb{R}^{N \times N}$ can be divided into three steps.

At first, we construct a check matrix of QC-LDPC codes using the construction method in [22], setting row weight and column weight of the matrix to be 8. The check matrix of the QC-LDPC codes is jointly determined by the base matrix and the shift matrix. The size of base matrix and the size of shift matrix are both 8×8. The check matrix is also divided equally into 8×8 parts. Each element of the base matrix is 0 or 1. The position of check matrix corresponding to the 0 of base matrix will be an all-zero matrix. In contrast, the position of the check matrix corresponding to the 1 of the base matrix will be a cyclically right-shifting identity matrix. The base matrix $\boldsymbol{G_b}$ is set to be an all-one matrix of 8×8 as Equation (5):

$$\boldsymbol{G_b} = \begin{pmatrix} 1 & 1 & \cdots & 1 \\ 1 & 1 & \cdots & 1 \\ \vdots & \vdots & \ddots & \vdots \\ 1 & 1 & \cdots & 1 \end{pmatrix}_{8 \times 8.} \tag{5}$$

Therefore, each part of check matrix is a circulant permutation matrix obtained by cyclically right-shifting the identity matrix by p_{ij} positions expressed as $I^{p_{ij}}$, where I is the identity matrix and p_{ij} is the shifting value. The right-shifting value can be decided by the corresponding element of the shift matrix. Using the construction method of QC-LDPC codes, we can get a shift matrix as Equation (6):

$$\boldsymbol{G_s} = \begin{pmatrix} p_{11} & p_{12} & \cdots & p_{18} \\ p_{21} & p_{22} & \cdots & p_{28} \\ \vdots & \vdots & \ddots & \vdots \\ p_{81} & p_{82} & \cdots & p_{88} \end{pmatrix}_{8 \times 8,} \tag{6}$$

where $p_{ij} (0 \leq i \leq 8, 0 \leq j \leq 8)$ denotes the shift value of the identity matrix. By combining base matrix and shift matrix, we can get the check matrix H as Equation (7):

$$\boldsymbol{H} = \begin{pmatrix} I^{p_{11}} & I^{p_{12}} & \ldots & I^{p_{17}} & I^{p_{18}} \\ I^{p_{21}} & I^{p_{22}} & \ldots & I^{p_{27}} & I^{p_{28}} \\ \vdots & \vdots & \ddots & \vdots & \vdots \\ I^{p_{71}} & I^{p_{72}} & \ldots & I^{p_{77}} & I^{p_{78}} \\ I^{p_{81}} & I^{p_{82}} & \ldots & I^{p_{87}} & I^{p_{88}} \end{pmatrix} \tag{7}$$

where $I^{p_{ij}}$ is a $N/8 \times N/8$ $(0 \leq p_{ij} \leq N/8)$ circulant permutation matrix. It is matrix which doesn't exists four rings.

The second step is replacing the value of the non-zero position in H with the weight set of RCM according to the three constraints in Section 2. Since each $I^{p_{ij}}$ is obtained by a right-shifting identity matrix, there are only eight non-zero positions for each row and column of the matrix H. There must be a non-zero position in each row of $I^{p_{ij}}$. These two factors are helpful conditions for constructing the mapping matrix. Therefore, we combine two adjacent $I^{p_{ij}}$ of each row into one block, denoted as $g_{ab} = [I^{p_{a(2b-1)}}, I^{p_{a(2b)}}] (1 \leq a \leq 8, 1 \leq b \leq 4)$.

The last step is to divide the different weights into three groups denoted as $\{+1, -1\}$, $\{+2, -2\}$ and $\{+4, -4\}$. Each g_{ab} is assigned to a definite group of weights. According to the conventional mapping matrix, g_{ab} chooses weight set as Equation (8) (shown at the top of next page). Each row of each block has two non-zero positions. For different elements in the same group, the two weights are

assigned to the two non-zero positions with equal probability. In this way, we can construct a mapping matrix without four rings, while satisfying the three constraints of RCM [8].

$$G_{new} = \begin{bmatrix} g_{11}\{+4,-4\} & g_{12}\{+4,-4\} & g_{13}\{+2,-2\} & g_{14}\{+1,-1\} \\ g_{21}\{+2,-2\} & g_{22}\{+1,-1\} & g_{23}\{+4,-4\} & g_{24}\{+4,-4\} \\ g_{31}\{+4,-4\} & g_{32}\{+4,-4\} & g_{33}\{+1,-1\} & g_{34}\{+2,-2\} \\ g_{41}\{+1,-1\} & g_{42}\{+2,-2\} & g_{43}\{+4,-4\} & g_{44}\{+4,-4\} \\ g_{51}\{+4,-4\} & g_{52}\{+4,-4\} & g_{53}\{+2,-2\} & g_{54}\{+1,-1\} \\ g_{61}\{+2,-2\} & g_{62}\{+1,-1\} & g_{63}\{+4,-4\} & g_{64}\{+4,-4\} \\ g_{71}\{+4,-4\} & g_{72}\{+4,-4\} & g_{73}\{+1,-1\} & g_{74}\{+2,-2\} \\ g_{81}\{+1,-1\} & g_{82}\{+2,-2\} & g_{83}\{+4,-4\} & g_{84}\{+4,-4\} \end{bmatrix} \quad (8)$$

4. Improved Belief Propagation Algorithm

This section contains two parts. In the following, we first introduce the improved belief propagation (IBP) which is based on the threshold of the soft information. Next, we will analyze the error probability of soft information.

4.1. Introduction of Improved Belief Propagation

One advantage of RCM as an adaptive transmission system is that the transmitter does not require precise channel estimation feedback from the receiver. The transmitter transfers the next data block after receiving an acknowledgement (ACK) from the receiver. The specific model of transmitter is shown in Figure 1. A major feature of the transmitter is that it constantly increases the transmitted symbols for the same data block when no ACK is received. It achieves an adaptive code rate via adjusting the number of transmitted symbols.

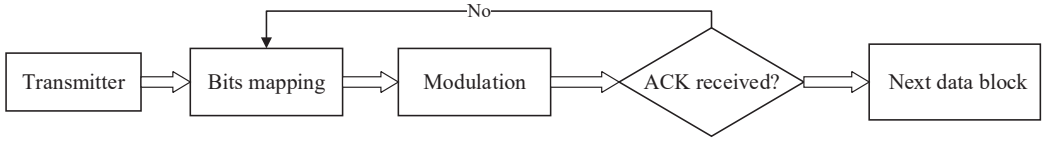

Figure 1. Transmission model of the transmitter.

As for the original receiver, it will continue to receive symbols when it fails to pass the cyclic redundancy check (CRC). In addition, the ACK signal will not be sent to the transmitter. As for the newly received symbols, they are put together with the previously received symbols for decoding. The receiver continuously repeats the two procedures of decoding and receiving symbols. This step will not stop until the CRC is passed. The receiver will feed back an ACK to the transmitter when CRC passes. The specific model of original receiver is shown in Figure 2a.

In the original model, soft information by the last decoding is completely discarded when the CRC is failed. However, in many cases, most of the soft information by the last decoding is correct. Only a small number of errors occur. Therefore, the efficiency of decoding is greatly reduced due to the large loss of valid information. IBP aims to retain as much valid information as possible

RCM initially uses a belief propagation (BP) algorithm in [8] as the decoding algorithm. In [9], the maximum likelihood ratio BP (LLR-BP) decoding algorithm is proposed, which effectively accelerated decoding and reduced the complexity of the hardware. In the LLR-BP algorithm, the soft information is the LLR and each final decision depends on the LLR acquired by iterative decoding. The judgment rules are as follows. The final soft information which is larger than or equal to 0 is judged as information bit "1". Thus, the soft information less than 0 is judged as information bit "0". There is a very important property of the LLR-BP algorithm that the soft information, of which the absolute values are very large, has a small error probability of judgment. This property will be proven in Section 4.2. Based on this property, we proposed an improved belief propagation (IBP) decoding algorithm.

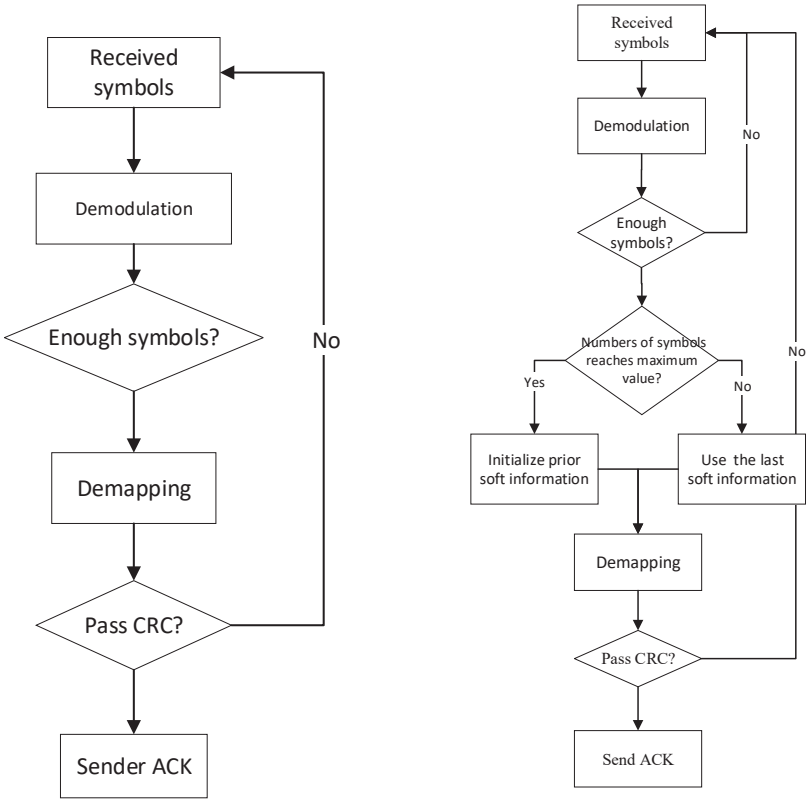

Figure 2. Comparison between original receiver model and improved receiver model. (**a**) Original receiver model. (**b**) Improved receiver model.

Due to the low error probability of judgment of larger value, the IBP sets a threshold of absolute value when the CRC fails. The portion of the soft information that is higher than the threshold is reserved. In contrast, the portion of soft information below the threshold is discarded. The reserved soft information is taken as the initial information at the beginning of the next iteration.

To keep the improved system stable and effective, we set the maximum value for the number of received symbols. The specific operation of setting the maximum value is as follows. When the maximum number of received symbols is not reached, we use the IBP algorithm to reserve the soft information whose absolute value is greater than the threshold. In contrast, When the maximum number of received symbols is reached and the CRC is still not passed, we will not reserve the soft information. Such a system design not only ensures the stability of the system, but also improves the efficiency of system decoding. The specific improved receiver model is shown in Figure 2b.

4.2. Analysis of Error Probability of Soft Information

At present, the additive white Gaussian noise (AWGN) channel model is mainly considered by RCM. Suppose the received symbol vector is $\boldsymbol{r} \in \mathbb{R}^{M\times 1}$. $\boldsymbol{r}$ is denoted as follow:

$$\boldsymbol{r} = \boldsymbol{G} \cdot \boldsymbol{x} + \boldsymbol{e}, \tag{9}$$

where $\boldsymbol{e} \in \mathbb{R}^{M\times 1}$, $e_i \in \boldsymbol{e}$ and $e_i \sim \mathcal{N}(0, \sigma^2)$. The task of receiver is finding out the source bits with the maximum a posterior (MAP) probability. In [8], belief propagation algorithm has been used

for decoding which is initially proposed in [23] for sparse signal recovery of compressive sensing. The decoding process is to find the optimal solution for the following problem:

$$\hat{\boldsymbol{x}} = argmax\ p(\boldsymbol{x}|\boldsymbol{r}). \tag{10}$$

For the RCM, the BP iterative decoding algorithm is used. The process of iterative decoding repeatedly updates the variable nodes and the symbol nodes through the information exchange between the symbol nodes and the variable nodes. Suppose r_i is the received symbol and $r_i \in \boldsymbol{r}$. As Figure 3 shows, the set of variable nodes $\boldsymbol{x_i} = \{x_{i_1}, x_{i_2}, \cdots, x_{i_L}\}$ are connected to the symbol node r_i. The number of the weight is L, $\boldsymbol{W_s} = \{w_1, w_2, w_3, \cdots, w_L\}$. The information transmitted by the symbol node to the variable nodes x_{i_k} is $v_{i_k} = p(r_i|x_{i\backslash k})$, where $x_{i\backslash k}$ denotes the set of variable nodes connected to the symbol node r_i excluding x_{i_k}.

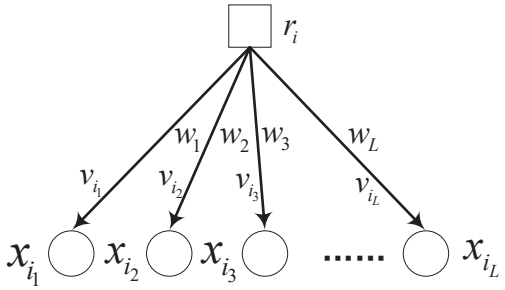

Figure 3. Symbol node conveys message to its all neighboring variable nodes.

The two conditional probability function sent by the symbol node to the variable nodes are as follow:

$$\begin{aligned} v_{i_k}^{(0)} &= p(r_i|x_{i_k} = 0) \\ &= \sum_{s=s_{i\backslash k_{\min}}}^{s_{i\backslash k_{\max}}} p(s_{i\backslash k} = s) \cdot \frac{1}{\sqrt{2\pi}\sigma} \cdot e^{-\frac{(r_i - s)^2}{2\sigma^2}}, \end{aligned} \tag{11}$$

$$\begin{aligned} v_{i_k}^{(1)} &= p(r_i|x_{i_k} = 1) \\ &= \sum_{s=s_{i\backslash k_{\min}}}^{s_{i\backslash k_{\max}}} p(s_{i\backslash k} = s) \cdot \frac{1}{\sqrt{2\pi}\sigma} \cdot e^{-\frac{(r_i - s - w_k)^2}{2\sigma^2}}, \end{aligned} \tag{12}$$

where $s_{i\backslash k} = \sum_{d=1, d\neq k}^{L} w_d x_{i_d}$, $s_{i\backslash k_{\min}}$ and $s_{i\backslash k_{\max}}$ represent the maximum and minimum values of $s_{i\backslash k}$ respectively.

As Figure 4 shows, the set of symbol nodes $\boldsymbol{r_j} = \{r_{j_1}, r_{j_2}, \cdots, r_{j_n}\}$ are connected to the variable nodes x_j. The information transmitted by the variable node to the symbol nodes is $u_{j_k} = p(x_j|r_{j/k})$, where $r_{j/k}$ denotes the set of the symbol nodes connected to the variable node x_j excluding r_{j_k}.

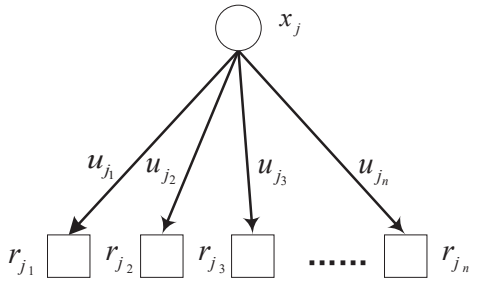

Figure 4. Variable node conveys message to its all neighboring symbol nodes.

The two conditional probability function passed to the symbol nodes by the variable node are as follow:

$$u_{j_k}^{(0)} = p(x_j = 0|r_{j\backslash k}) = \frac{\prod_{m=1,m\neq k}^{n} p(r_{j_m}|x_j = 0)}{\sum_{b\in\{0,1\}} \prod_{m=1,m\neq k}^{n} p(r_{j_m}|x_j = b)}, \tag{13}$$

$$u_{j_k}^{(1)} = p(x_j = 1|r_{j\backslash k}) = \frac{\prod_{m=1,m\neq k}^{n} p(r_{j_m}|x_j = 1)}{\sum_{b\in\{0,1\}} \prod_{m=1,m\neq k}^{n} p(r_{j_m}|x_j = b)}. \tag{14}$$

The transmitted symbols through the AWGN channel are independent of noise. As for transmitted symbol s and received symbol r_i , the conditional probability function of the channel can be expressed as:

$$p(r_i|s) = \frac{1}{\sqrt{2\pi}\sigma} \cdot e^{-\frac{(r_i-s)^2}{2\sigma^2}}. \tag{15}$$

Taking the LLR-BP in the decoding is equivalent to taking the logarithm of the conditional probability function of the channel.

$$\ln p(r_i|s) = \ln \frac{1}{\sqrt{2\pi}\sigma} - \frac{(r_i - s)^2}{2\sigma^2}, \tag{16}$$

where $r_i - s = e_i$. The specific operation of BP-LLR is as follow. In the decoding of symbol nodes of the BP algorithm, symbol nodes transmit a message including $v_{i_k}^{(0)}$ and $v_{i_k}^{(1)}$ to variable nodes as Equations (11) and (12). Using LLR, The transmitted message $v_{i_k}^{l}$ will become the logarithmic form as follow:

$$v_{i_k}^{l} = \ln\left(\frac{v_{i_k}^{(0)}}{v_{i_k}^{(1)}}\right). \tag{17}$$

In the decoding of variable nodes, variable nodes transmit a message include $u_{i_k}^{(0)}$ and $u_{i_k}^{(1)}$ to variable node as Equations (13) and (14). Using LLR, it only needs to add an operation rather than multiplication. The information $u_{j_k}^{(l)}$ of variable nodes transmitted to symbol nodes is denoted as:

$$u_{j_k}^{l} = \ln\left(\frac{u_{j_k}^{(0)}}{u_{j_k}^{(1)}}\right) = \sum_{j_k\neq i_k} \ln\left(\frac{v_{i_k}^{(0)}}{v_{i_k}^{(1)}}\right). \tag{18}$$

In LLR-BP, the LLR $u_{j_k}^{l}$ is the soft information acquired by iterative decoding. The decision process is as follow:

$$b = \begin{cases} 1, & u_{j_k}^{l} < 0; \\ 0, & u_{j_k}^{l} \geq 0; \end{cases} \tag{19}$$

Combining (11) and (12), $v_{i_k}^{l}$ is further represented as:

$$\begin{aligned} v_{i_k}^{l} &= \sum_{s=s_{i\backslash k_{min}}}^{s_{i\backslash k_{max}}} \ln s - \sum_{s=s_{i\backslash k_{min}}}^{s_{i\backslash k_{max}}} \frac{(r_i - s)^2}{2\sigma^2} - \sum_{s=s_{i\backslash k_{min}}}^{s_{i\backslash k_{max}}} \ln s + \sum_{s=s_{i\backslash k_{min}}}^{s_{i\backslash k_{max}}} \frac{(r_i - s - w_k)^2}{2\sigma^2} \\ &= \sum_{s=s_{i\backslash k_{min}}}^{s_{i\backslash k_{max}}} \frac{{w_k}^2 - 2w_k(r_i - s)}{2\sigma^2} = \sum \frac{w_k}{2\sigma^2} - \frac{w_k}{\sigma^2} \sum_{s=s_{i\backslash k_{min}}}^{s_{i\backslash k_{max}}} (r_i - s) \end{aligned}. \tag{20}$$

r_i is the received symbol and s represents the possible transmitted symbol, $r_i - s$ can be simplified to $e_i + d$, where e_i is the noise and d represents different values among possible symbols. Due to the reason that these possible transmitted symbols are accurate, d can be seen as a constant. w_k and σ^2 both can be seen as constants. Let A represent an additive constant and let p represent a multiplier constant. We can further simplify $v_{j_k}^l$.

$$v_{i_k}^l = A + p \cdot \sum e_i. \tag{21}$$

e_i satisfies Gaussian distribution. As can be found from Equation (21), $v_{i_k}^l$ satisfies a distribution obtained by linear operation of Gaussian distribution. During the decoding, the variable nodes only perform the add operation $u_{j_k}^l$ is also a linear function of e_i as Equation (22):

$$u_{j_k}^l = \sum \left\{ A + p \cdot \sum e_i \right\}. \tag{22}$$

According to the above analysis, the distribution of soft information is closed to Gaussian distribution. According to the property, the closer the absolute value of soft information is to 0, the greater the error probability of soft information. This property is helpful in the selection of thresholds.

5. Simulation

In this section, we first obtain the threshold of soft information through simulation. Then, we compare the performance of MMwoFR and IBP with the original RCM. We also have compared the complexity of the improved scheme. In order to evaluate the stability of the improved scheme, we also have performed a sensitivity analysis.

5.1. Threshold of Soft Information

In a practical system, a receiver should choose a suitable threshold. When the threshold is too large, less valid soft information is retained. Conversely, if the threshold is too small, the retained error soft information will increase. We have previously summarized the distribution of wrong soft information. It is verified below.

Simulation is performed at SNR from 5 dB to 30 dB. In the experiment, we choose 10^5 bits as a block and run 10,000 blocks for each SNR. For each block of bits, we find the soft information corresponding to error bits. Then, we got the probability density function (PDF) of these soft information values and averaged the 300 blocks to get the means. Figure 5 shows the PDF of wrong soft information values when SNR = 5 dB, 10 dB, 15 dB, 20 dB, 25 dB and 30 dB. It also shows that the probability will decrease when the soft information value is far from 0.

In order to obtain reliable thresholds, the cumulative distribution function (CDF) of soft information corresponding to error bits has been obtained according to the simulation results. According to the CDF, select the point corresponding to the probability at about 99% as the threshold. The final selected threshold is at Table 1.

Table 1. Thresholds of soft information for different SNR.

SNR(dB)	5	6	7	8	9	10	11	12	13
Threshold	8.06	7.57	7.35	6.90	6.81	6.5	6.34	6.17	6.00
SNR(dB)	14	15	16	17	18	19	20	21	22
Threshold	5.91	5.80	5.33	5.14	4.67	4.47	4.25	4.13	4.04
SNR(dB)	23	24	25	26	27	28	29	30	
Threshold	3.91	3.75	3.55	3.46	3.40	3.24	3.10	3.07	

At the end of each iteration, the remaiing soft information is scaled down according to the threshold value so that the maximum value of soft information retained each time would not exceed the threshold.

Although these thresholds are based on simulations, they are not sensitive within a certain range. We also have done simulation analysis of sensitivity of the thresholds. The results will be shown in Section 5.4.

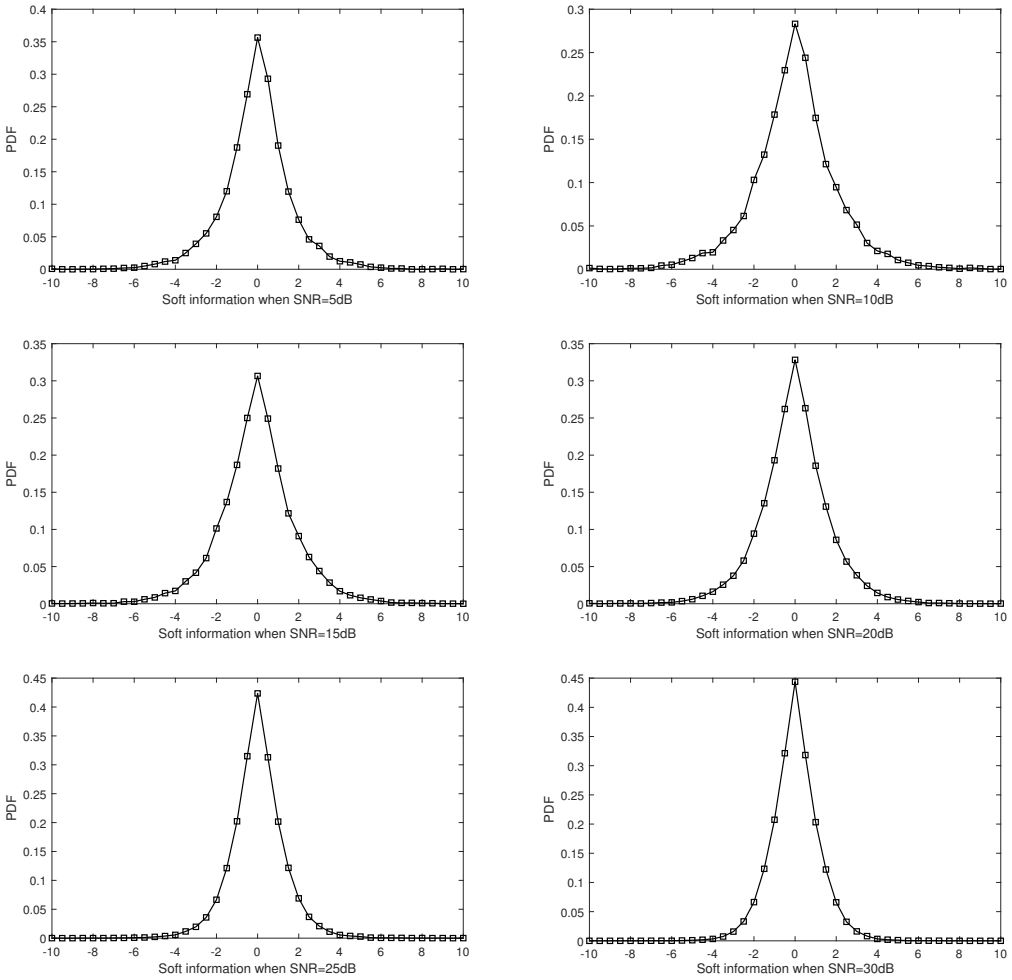

Figure 5. Probability density function of wrong soft information.

5.2. Performance Evaluation

In order to confirm the improved scheme's performance, a lot of experiments are performed in this section. Utilizing the mapping matrix without four rings (MMwoFR) and improved belief propagation (IBP) algorithm, we implement four different situations. The first is the original RCM. The second only uses the MMwoFR. The third only uses the IBP. The last combines MMwoFR and IBP (MMwoFR-IBP). The presentation of these four situations will be more intuitive to the comparison of the performance of different schemes.

The weight set of the original RCM is $\{\pm 1, \pm 2, \pm 4, \pm 4\}$. In [13,15], the weight sets $\{\pm 1, \pm 2, \pm 4, \pm 8\}$ and $\{\pm 1, \pm 1, \pm 2, \pm 2\}$ have been discussed for RCM. In order to show the universality of the improved scheme, we take experimental simulations using the three weight sets (shown in Table 2). It can be found from Table 2 that different weight sets have different elements; therefore, the classes of generated symbols are different.

Table 2. Three weight sets of RCM.

Name	Weight Set	L	Type of Symbol
RCM1	$\{\pm1, \pm1, \pm2, \pm2\}$	8	13
RCM2	$\{\pm1, \pm2, \pm4, \pm4\}$	8	23
RCM3	$\{\pm1, \pm2, \pm4, \pm8\}$	8	31

Simulation is performed under the AWGN channel. Every 400 bits are a block. The dimension of mapping matrix is designed as 400×400. When the channel conditions are very poor, the number of generated symbols may exceed 400. At this time, the mapping matrix is repeated. Symbols generated by the same row of mapping matrix are merged using the maximum merger ratio.

During transmission, the demapping threshold is the same as the original RCM [8]. When CRC is failed, the receiver will increase the received symbols. In the original receiver model, the additional number of symbols is 10. As for IBP, less additional symbols may succeed during decoding due to the retention of soft information . However, the number of decoding will increase when the additional number of symbols is reduced. Therefore, the additional number of symbols is chosen based on the performance and the number of decoding. We simulated the performance of MMwoFR-IBP when the additional number is in the range of 1–10. According to the result of simulations, we choose the additional number which has the best performance. When the performance is equivalent, we choose the additional number which has less number of decoding. According to the above selection, the number of additional symbols is shown in Table 3.

Table 3. Additional number of symbols for different SNR.

SNR(dB)	5	6	7	8	9	10	11	12	13
Number	10	10	10	10	10	10	10	10	10
SNR(dB)	14	15	16	17	18	19	20	21	22
Number	7	7	7	5	5	5	3	3	3
SNR(dB)	23	24	25	26	27	28	29	30	
Number	2	2	2	1	1	1	1	1	

In order to maintain a more stable system, a maximum number of received symbols is set. When the number of received symbols is lower than the maximum number, the soft information will be retained. In contrast, when the number of received symbols is higher than the maximum number, all the soft information will be discarded. In [8], the cumulative distribution function (CDF) of successful decoding at different SNR has been obtained. In our simulations, we ran 1000 blocks of data. In this case, we can get 1000 numbers of symbols for successful decoding at each SNR. We choose the maximum number in the 1000 numbers as the threshold of the maximum number of symbol. The maximum number of symbols for each SNR is shown in Table 4.

Table 4. Maximum number of received symbols for different SNR.

SNR(dB)	5	6	7	8	9	10	11	12	13
Number	2650	2100	1280	1100	980	770	710	450	350
SNR(dB)	14	15	16	17	18	19	20	21	22
Number	300	290	260	240	230	200	190	170	170
SNR(dB)	23	24	25	26	27	28	29	30	
Number	170	150	150	150	150	150	150	140	

In order to evaluate the performance, we use goodput as the evaluation metric, which is the rate of correctly received bits. The goodput performance of different weight sets is shown in Figures 6–8. When the weight set is $\{\pm1, \pm1, \pm2, \pm2\}$, RCM1 achieves the rate of 4.81 bits/s/Hz at 27 dB, while MMwoFR achieves the same rate at 25 dB, IBP at 26 dB and MMwoFR-IBP at 24 dB. MMwoFR-IBP's most goodput reaches 5.28 bits/s/Hz and achieves 9.1% goodput gain.

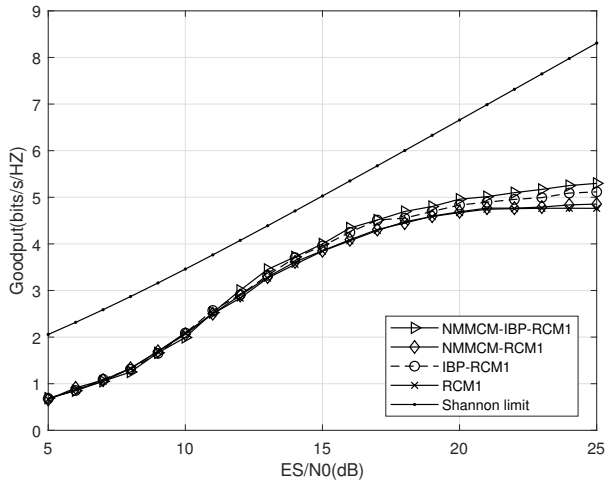

Figure 6. Goodput comparison in different system with weight set $\{\pm 1, \pm 1, \pm 2, \pm 2\}$.

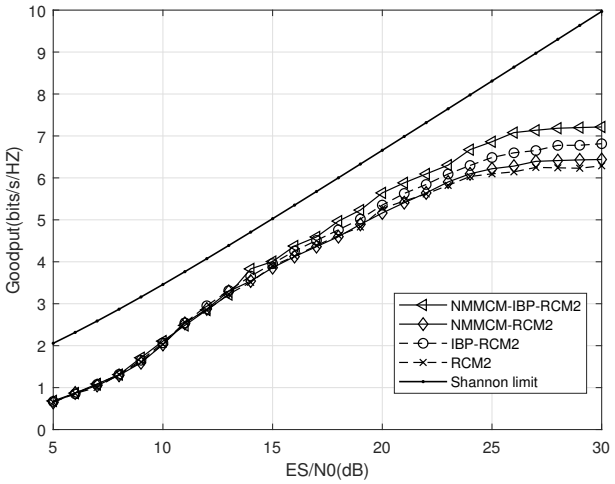

Figure 7. Goodput comparison in different system with weight set $\{\pm 1, \pm 2, \pm 4, \pm 4\}$.

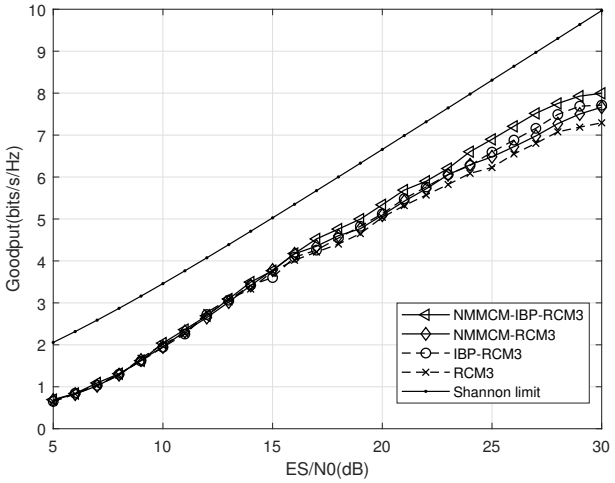

Figure 8. Goodput comparison in different system with weight set $\{\pm 1, \pm 2, \pm 4, \pm 8\}$.

When the weight set is $\{\pm1, \pm2, \pm4, \pm4\}$, RCM2 achieve the rate of 6.25 bits/s/Hz at 30 dB, while MMwoFR achieve the same rate at 27 dB, IBP at 24 dB and MMwoFR-IBP at 23 dB. MMwoFR-IBP's most goodput reaches 7.29 bits/s/Hz and achieves 16.3% goodput gain.

When the weight set is $\{\pm1, \pm2, \pm4, \pm8\}$, RCM3 achieves the rate of 7.3 bits/s/Hz at 30 dB, while MMwoFR achieves the same rate at 28 dB, IBP at 28 dB and NMMCM-IBP-RCM2 at 26 dB. MMwoFR-IBP's most goodput reaches 7.96 bits/s/Hz and achieves 7.2% goodput gain. As depicted from the curve in the figure, the performance of MMwoFR-IBP is optimal. Both MMwoFR and IBP can improve the spectrum efficiency. As the SNR increases, the increment of spectrum efficiency will be more obvious, and especially apparent at high SNR.

Through the comparison of performance of four situations, we find that MMwoFR-IBP, MMwoFR and IBP are all superior to the original RCM at high-SNR range. The reason resides in the following two points. First, when using MMwoFR, the speed of transmission and update of the soft information in the iterative decoding is accelerated. The result of demapping is more reliable. Second, the IBP algorithm retained valid information which is discarded for the original RCM. These valid information as initial information of next decoding will increase the correct probability of decoding so that the number of symbols required for decoding is reduced. The two points are both beneficial to the improvement of spectrum efficiency.

5.3. Comparison of Complexity

The iteration decoding algorithm of RCM is complex. The complexity mainly depends on the process of decoding. In the decoding, the complexity of the process of symbol nodes dominates. Existing improved decoding algorithms all aim to simplify the process of symbol nodes. When weight set is settled the same, the complexity of decoding depends just on the decoding number at each round. Under the condition that they use the same weight sets, the complexity of four schemes can be compared by the decoding number.

Figure 9 shows the average number of decoding for the original RCM, MMwoFR, IBP and MMwoFR-IBP with the weight sets $\{\pm1, \pm2, \pm4, \pm4\}$. As can be seen from the figure, the average decoding number at low SNR is much higher than that at high-SNR and the average decoding number of four schemes is comparable at low SNR. Due to the reason that the additional number of symbol is reduced, the complexity of IBP and MMwoFR-IBP is slightly higher than the original RCM and MMwoFR at high SNR. Overall, the complexity is comparable.

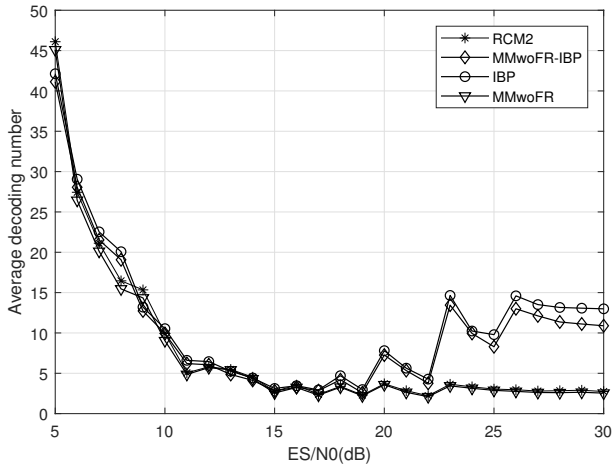

Figure 9. Average decoding number under different SNR with weight set $\{\pm1, \pm2, \pm4, \pm4\}$.

5.4. Sensitivity to SNR Estimation Error

In practical communication systems, the threshold will change as SNR changes. However, existing channel estimation techniques do not usually achieve accurate and real-time channel information. One obvious advantage of the original RCM is that it does not need accurate channel information. Therefore, it is necessary to evaluate whether the proposed scheme is sensitive to inaccurate SNR estimated value. According to [24], 98% of the SNR estimation error is within -6 dB to 6 dB. Therefore, our sensitivity analysis is within this range.

In the simulation, we chose four situations of 10 dB, 15 dB, 20 dB and 25 dB. Assume the estimated error within -6 dB to 6 dB $\times 10^7$ bits were used in the experiment. The experimental results are shown in Figure 10. It can be found that the goodput performance has small fluctuation. According to the simulation result, we conclude that the proposed schemes are not sensitive to the SNR estimation error. It is crucial for the proposed scheme to adapt the actual communication environment.

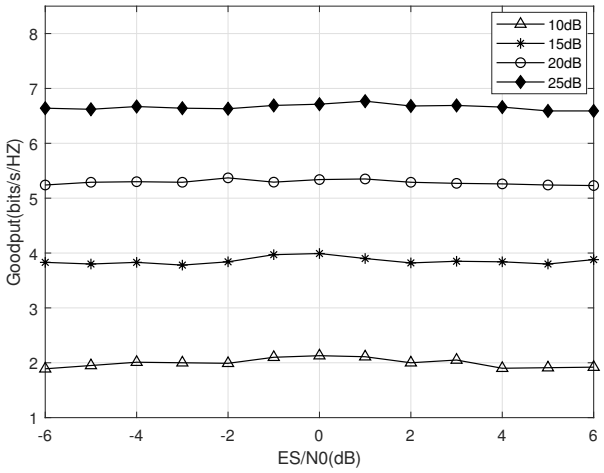

Figure 10. Sensitivity to SNR estimation errors.

6. Conclusions

In this paper, a new mapping matrix construction method of RCM is proposed. This method is able to construct the mapping matrix without four rings (MMwoFR), which improves the update rate of information between symbol nodes and variable nodes during decoding. Based on the LLR-BP decoding algorithm, an improved belief propagation (IBP) decoding algorithm which uses soft information by last decoding is proposed. When the CRC is failed, the soft information from the last decoding, which is higher than the threshold, is reserved as the initial information of the following decoding, which greatly improves the decoding efficiency. Simulation shows that these two methods achieve great goodput gain. We have evaluated the performance of MMwoFR, IBP and the combination of both (MMwoFR-IBP) in the additive white Gaussian noise (AWGN) channel. Compared to the original RCM, these three schemes all achieved performance gain at high SNR. MMwoFR achieves about 3% goodput gain within the SNR region from 25 dB to 30 dB. IBP achieves at least 3% goodput gain from 14 dB to 30 dB and achieves a maximum goodput gain of 8% at 30 dB. Especially, using MMwoFR-IBP achieves at least 12% goodput gain from 25 dB to 30 dB and achieves 16% goodput gain at 30 dB. In the future, we aim to further research RCM and the transmission system.

Author Contributions: Experiments were conceived and designed by J.Z., W.L. (Wei Liu), Z.P.; Experiments were performed by J.Z., W.L. (Wei Liu), Z.P.; Results were analyzed by all authors. All authors were involved in paper writing.

Funding: This research received no external funding.

Acknowledgments: The authors would like to thank editors and reviewers for many constructive suggestions and comments that helped to improve the quality of the paper.

Conflicts of Interest: The authors declare no conflicts of interest.

References

1. Goeckel, D.L. Adaptive coding for time-varying channels using outdated fading estimates. *IEEE Trans. Commun.* **1999**, *47*, 844–855. [CrossRef]
2. Song, K.B.; Ekbal, A.; Chung, S.T.; Cioffi, J.M. Adaptive modulation and coding (AMC) for bit-interleaved coded OFDM (BIC-OFDM). *IEEE Int. Conf. Commun.* **2006**, *6*, 3197–3201.
3. Tong, J.; Ping, L.; Ma, X. Superposition Coded Modulation With Peak-Power Limitation. *IEEE Trans. Inf. Theory* **2009**, *55*, 2562–2576. [CrossRef]
4. Shokrollahi, A. Raptor codes. *IEEE Trans. Inf. Theory* **2006**, *52*, 2551–2567. [CrossRef]
5. Luby, M. LT codes. In Proceedings of the Symposium on Foundations of Computer Science, Vancouver, BC, Canada, 16–19 November 2002; pp. 271–280.
6. Perry, J.; Iannucci, P.A.; Fleming, K.E.; Balakrishnan, H.; Shah, D. Spinal codes. *ACM SIGCOMM Comput. Commun. Rev.* **2012**, *42*, 49–60. [CrossRef]
7. Shirvanimoghaddam, M.; Li, Y.; Vucetic, B. Near-Capacity Adaptive Analog Fountain Codes for Wireless Channels. *IEEE Commun. Lett.* **2013**, *17*, 2241–2244. [CrossRef]
8. Cui, H.; Luo, C.; Tan, K.; Wu, F.; Chen, C.W. Seamless rate adaptation for wireless networking. In Proceedings of the International Symposium on Modeling Analysis and Simulation of Wireless and Mobile Systems, MSWIM 2011, Miami, FL, USA, 31 October–4 November 2011; pp. 437–446.
9. Rao, W.; Dong, Y.; Lu, F.; Wang, S. Log-likelihood ratio algorithm for rate-compatible modulation. In Proceedings of the IEEE International Symposium on Circuits and Systems, Beijing, China, 19–23 May 2013; pp. 1938–1941.
10. Cui, H.; Luo, C.; Wu, J.; Chen, C.W.; Wu, F. Compressive Coded Modulation for Seamless Rate Adaptation. *IEEE Trans. Wirel. Commun.* **2013**, *12*, 4892–4904. [CrossRef]
11. Lu, F.; Dong, Y.; Rao, W.; Chen, C.W. Low Complexity Decoding Algorithms for Rate Compatible Modulation. *IEEE Access* **2018**, *6*, 31417–31429. [CrossRef]
12. Lu, F.; Dong, Y.; Rao, W. A Parallel Belief Propagation Decoding Algorithm for Rate Compatible Modulation. *IEEE Commun. Lett.* **2017**, *21*, 1735–1738. [CrossRef]
13. Wu, J.; Teng, Z.; Cui, H.; Luo, C.; Huang, X.; Chen, H.H. Arithmetic-BICM for Seamless Rate Adaptation for Wireless Communication Systems. *IEEE Syst. J.* **2016**, *10*, 228–239. [CrossRef]
14. Duan, R.; Liu, R.; Shirvanimoghaddam, M.; Li, Y.; Chen, C.W. A Low PAPR Constellation Mapping Scheme for Rate Compatible Modulation. *IEEE Commun. Lett.* **2016**, *20*, 256–259. [CrossRef]
15. Rao, W.; Dong, Y.; Chen, S.; Lu, F.; Wang, S. An Efficient Rate Compatible Modulation with Variable Weight Sets. *IEEE Access* **2018**, *6*, 5064–5074. [CrossRef]
16. Wang, M.; Wu, J.; Yu, W.; Wang, H.; Li, J.; Shi, J.; Luo, C. Efficient coding modulation and seamless rate adaptation for visible light communications. *IEEE Wirel. Commun.* **2015**, *22*, 86–93. [CrossRef]
17. Shirvanimoghaddam, M.; Li, Y.; Dohler, M.; Vucetic, B.; Feng, S. Probabilistic Rateless Multiple Access for Machine-to-Machine Communication. *IEEE Trans. Wirel. Commun.* **2015**, *14*, 6815–6826. [CrossRef]
18. Gallager, R. Low-density parity-check codes. *IRE Trans. Inf. Theory* **1962**, *8*, 21–28. [CrossRef]
19. Kou, Y.; Lin, S.; Fossorier, M.P.C. Low-density parity-check codes based on finite geometries: A rediscovery and new results. *IEEE Trans. Inform. Theory* **2001**, *47*, 2711–2736. [CrossRef]
20. Fan, J.L. Array codes as LDPC codes. In *Constrained Coding and Soft Iterative Decoding*; Springer: Berlin, Germany, 2001; pp. 195–203.
21. Tanner R.M.; Sridhara D.; Fuja T. A class of group-structured LDPC codes. In Proceedings of the International Symposium on Communication Theory Applications, Ambleside, UK, 15–20 July 2001.
22. Wang, Y.; Yedidia, J.S.; Draper, S.C. Construction of high-girth QC-LDPC codes. In Proceedings of the International Symposium on Turbo Codes and Related Topics, Lausanne, Switzerland, 1–5 September 2008; pp. 180–185.

23. Baron, D.; Sarvotham, S.; Baraniuk, R.G. Bayesian Compressive Sensing Via Belief Propagation. *IEEE Trans. Signal Process.* **2009**, *58*, 269–280. [CrossRef]
24. Edalat, F.; Edalat, F.; Katabi, D.; Sodini, C.G. Frequency-aware rate adaptation and MAC protocols. In Proceedings of the International Conference on Mobile Computing and NETWORKING, Beijing, China, 20–25 September 2009; pp. 193–204.